

Optical Measurements in Production of Single Wall Carbon Nanotubes by Laser Ablation

Sivaram Arepalli
GB Tech
Houston, Texas
and
Carl D. Scott
NASA Johnson Space Center
Houston, Texas

Abstract

Measurements are made of optical radiation from the luminous plume in a flow tube used to produce single wall carbon nanotubes by laser ablation of graphite. Included are spectroscopic measurements of emission from the plume and a photograph of the luminous reaction zone. Measurements include 10 μ s exposures for a spectral region of 310 to 630 nm taken at several times after single and two-laser pulses. In addition, time dependent measurements are made at a number of wavelengths that correspond to peaks in spectral distribution. The spectral measurements are made using an intensified charge coupled device (ICCD) with an effective spectral resolution of about 1.9 nm. There is strong emission from the C₂ Swan bands and possibly from C₃. No atomic lines could be seen in the wavelength range covered. The Swan bands seem to be superimposed on a significant continuum whose origin is not certain. Temperatures are estimated from ratios of intensities of Swan band features.

Introduction

There has been great interest in the production and characterization of single wall carbon nanotubes (SWNTs) because of possible applications in nanostructures,¹ super strong materials,² nanoelectronics,³ and hydrogen storage.⁴ A variety of processes have been used to produce them, including arcs,^{5,6} laser ablation,^{7,8} chemical vapor deposition⁹ (CVD), and pyrolysis.¹⁰ A review of potential applications of carbon nanotubes is presented at this conference.¹¹

Single wall carbon nanotubes are being produced at the NASA Johnson Space Center using the laser ablation process developed at Rice University.^{7,8} Details of the formation of SWNTs are not well understood, but empirical variations have helped to optimize production rates and nanotube yield and purity. It was found at Rice University^{7,8} that operating with two successive laser pulses, one at 532 nm followed 50 ns later by another at 1064 nm resulted in the best yield. They also found that production is best at an argon pressure of about 66.7 kPa. The design and composition of the graphite target is also important for good production; a smooth surface and about 1% each of cobalt and nickel seem to be optimal. These results were found mainly by parametric variations of conditions, by good intuition, and by serendipity. It has been speculated that the growth of nanotubes occurs from partially closed fullerenes held "open" by nano-sized particles of Co/Ni metal catalyst on which C₂ attaches. Since the feed stock is probably C₂ or some other small molecular weight carbon chain that condenses out of the vaporized carbon, we

look for it in the emission spectra of the laser produced ablation plume. We will use it as a gauge of how the reactions leading to the formation of SWNTs might proceed kinetically. Unfortunately, there have been no known successful attempts to measure the formation of SWNTs directly in-situ. Laser Raman spectroscopy has been useful for detecting them in the solid state, but it has not been used for gas phase measurements during production.

The objective of this work is to measure the evolution of observable emission from the plume and to infer information about the formation of carbon nanotubes. This paper discusses measurements made of emission in the ultraviolet and visible region of the spectrum. We will present qualitative photographic information, some quantitative results derived from spectral measurements taken at various times after the laser pulse, and time dependent measurements at various wavelengths. Correlations of these spectral data from a parametric study of SWNT production will be presented later.

Experiment

The apparatus for nanotube production by laser ablation, similar to the one used at Rice University,^{7,8} is shown in Fig. 1. The current configuration uses two pulsed Nd:YAG lasers to ablate a graphite target containing cobalt and nickel (1 atom % each). The flow tube and the target are maintained at 1473 K in a flowing argon atmosphere (100 sccm flow; 66.7 kPa pressure). This slow flow of argon (1 to 3 mm/s) purges ablation products downstream into the cooler zone where they condense onto the tube walls. Two 10 Hz high power pulsed lasers are used for the ablation process, operating at 1064 nm (IR) and 532 nm (green). The lasers (Spectra Physics, GCR-16RS, 370 mJ/pulse in IR and Continuum, 682-10, 370 mJ/pulse in green) are controlled by a digital delay generator (Stanford Research Systems, DG535) such that the time separation between the IR and green laser pulses is adjustable. For normal operation, the IR laser pulse follows the green pulse by 50 nanoseconds. Two remotely controlled laser safety shutters (nmLaser Products, LSO55S3W8) are used on each beam to block them when required. The beams then pass through beam expanding telescopes. The IR laser beam is then routed by reflection via two 45° mirrors (coated for 1064nm) after which it is transmitted through a 45° mirror used to route the green beam. This mirror is coated for 532 nm. The two laser beams are adjusted to travel colinearly onto an uncoated quartz right angle prism (shown in Enclosure 2) and impinge on the target as overlapping beams. A low power He-Ne laser mounted outside Enclosure 1 is used as an alignment laser. The prism is attached to a remotely controlled mirror mount (Newport Corp., MM2000-OPT-0808). It is used to generate a raster scan of the laser beams on the target in an attempt to maintain uniform material removal from the target surface.

The lasers are adjusted to have comparable beam sizes of about 5 mm using the telescopes mounted inside Enclosure 1. The beam sizes are measured using a laser beam analyzer (Spiricon, LBA-300PC) shown in Enclosure 2. Before each run, a 3° quartz wedge is introduced into the beam path of the lasers. The reflection from the front surface of wedge is then directed onto another 3°-wedge and the subsequent front surface reflection is recorded with a CCD through a stack of neutral density filters. The wedges are located such that the CCD is at the same distance as the target surface from the first wedge and represents the laser beam intensity distribution on the target. Before each run

the pulse energies are measured using a volume absorbing laser power meter (Scientech, 38-0101 with display unit 36-5002) introduced into the beam paths (Enclosure 3).

The targets used for this study were supplied by Rice University and were made by compressing a paste containing high purity graphite, metal catalysts and Dylon carbon cement. The target rods (1.27 cm diameter and 5 cm length) are then baked and cured at high temperature (1073 to 1473 K) in a flowing argon atmosphere. The targets are then placed on graphite rods with graphite cement and are then attached to a stainless steel rod that extends beyond the end flange of the flow tube via a vacuum feed through. The position of the stainless steel rod is controlled by four set screws that are used to center the target in the flow tube. The flow tube is a 56 mm diameter quartz tube (3 mm wall thickness) with a Brewster window (7.5 cm diameter, 6 mm thick quartz flat) on one of the end flanges. The Brewster window flange also contains a 25 mm diameter inner quartz tube (60 cm long) and the laser beams are contained within this 25 mm clearance. The end flanges are water cooled. A graphite ring is used to support the inner tube. The target is normally located about 6 mm from the end face of the inner tube.

There is a provision to independently control the argon flow inside the inner tube as well as in the annular region by using a MKS146C Pressure controller. The flow control is achieved using a control valve (MKS, SP009-86), a 1000 Torr Baratron gauge (MKS, 626A) and mass flow controllers (MKS, 1179A and 1259B). The outlet side of the flow tube is connected to a mechanical vacuum pump via a screen mesh, two fine filters (400 microns and 7 microns), and a manifold of valves. For normal operation, a flow of 100 sccm is maintained in the inner tube using the control valve path. For parametric studies several flow combinations (50 to 800 sccm) were used.

The flow tube assembly is maintained inside a 60 cm long oven (Lindberg/Blue, HTF55332C) which is heated to about 1473 K. The target is placed near the center of the oven. The two halves of the oven are separated by about 3 cm using thermal insulation blocks. A small block is machined to the contour of the step with three holes drilled to hold the optical fiber assembly and is placed near the center of the oven. On the opposite side of the oven, there is a similar block and can be used for absorption measurements. The optical fiber assembly consists of a plano-convex lens (1.25 cm diameter and 2.5 cm focal length) which focuses the light from the central part of the ablation plume onto the end of a 800 micron quartz fiber. The other end of the fiber is connected to a fiber optic adapter attached to a Spex 270M spectrograph. Two detectors are used for recording the emission spectra: a gateable intensified CCD with 1024x256 pixels (Princeton Instruments, 1024MLDG) and a photomultiplier tube (Hamamatsu Corp., R955). The ICCD output is recorded using software provided by Princeton Instruments that allows background subtraction and adjustable gated detection using a programmable pulse generator (Princeton Instruments, PG200). However, the background subtraction mode was not used here. Instead, two background signals were obtained with the same number of scans (100) as in the measured spectra. One was obtained before and the other after the spectral measurements. These two background signals were averaged before subtracting them from the measured spectra. Most of the spectra are recorded with 25 micron slit widths using a 300 line/mm grating blazed at 500 nm. With a 300 line/mm grating, a coverage of about 350 nm in a single exposure of the ICCD is possible. The resolution, taking into account the finite size of the intensifier channels, is about 1.9 nm and the

spacing between pixels is about 0.322 nm. All the spectra are intensity calibrated using a standard lamp (Eppley Laboratory, GE30AT24/13) whose calibration is traceable to the NIST. Wavelengths are calibrated using emission lines from low pressure mercury, neon, krypton and argon lamps.

Transient spectral data is collected by connecting the output of the R955 tube to a 32K channel transient digitizer (LeCroy Corp., TR8818A and 6010 with Catalyst 2.1) which gives a minimum of 10 ns channel width or sampling time. The response time of the system can be as low as 3 ns. We estimate that the time resolution of our measurements is about 20 ns, which was measured using a sharp rising gate pulse from a boxcar unit (SRS, SR250) and a digital delay generator (SRS, DDG535).

All transient and steady state data are collected with stationary laser beams at the center of the target. Data collection is initiated 60 to 90 seconds after the start of the laser beams to allow for thermalization of the target surface.

Observations and Measurements

Three measurement techniques for determining properties of the laser ablation process for carbon nanotube production are reported here. These techniques are 1) still and video photography, 2) wavelength resolved emission spectroscopy using a spectrometer with a gated intensified charge coupled device (ICCD) detector, and 3) transient spectral measurements using a spectrometer with a photomultiplier and a transient digitizer.

Photographic Observations

The first diagnostic technique, photography, was used to obtain estimates of the size and location of the visible plume. The luminous plume is confined to a small region near the surface of the target. It extends about one centimeter from the surface and seems to have ragged edges. Its duration is very short, less than one millisecond per pulse, as confirmed first by high speed video and then by transient emission measurements. The plume appears violet-white in color both from direct observation and from photographs. Fig. 3 shows a close up of the laser plume and part of the region inside the inner flow tube which is illuminated by the laser. This photograph was taken with a notch filter to remove scattered 532 nm laser radiation. It shows the luminous plume where high temperatures exist. Inside the 1-inch tube in the region to the left of the plume, there is a glow that appears to contain high temperature particles, probably heated to incandescence by the lasers. Calculations of particle absorption of laser energy (taking into account the complex index of refraction of the particles) show that a large fraction of each particle may vaporize, particularly by the 532 nm beam. The fraction vaporized is independent of particle size, as long as the particles are smaller than the laser wavelength.

Emission Spectral Distributions

The second diagnostic technique is wavelength-resolved emission spectroscopy. Spectra averaged over about 10 μ s were obtained in the spectral range of about 320 to 630 nm (Fig. 4). These spectra were obtained at delay times of 0.4, 10, and 25 μ s after the laser pulse. The predominant feature in these spectra is the C₂ Swan band emission system¹² that results from the transition $d^3\Pi_g - a^3\Pi_u$. The lower $a^3\Pi_u$ state is not the ground state,

but only 716 cm^{-1} above it. Fig. 4 shows spectra taken at various times. These spectra are normalized to the peak intensity at 516 nm, which is the $(v',v'')=(0,0)$ bandhead of the C_2 Swan band system. The peaks associated with various vibrational transitions, $\Delta v = v' - v''$, are indicated in Fig. 4, along with a tentative identification of C_3 emission. Fig. 5 shows similar spectra comparing that of single laser pulses, either “green” at 532 nm or “IR” at 1064 nm, with that produced by both the green and IR laser pulses in succession.

Comparisons of various laser pulses and delay times are shown in Figs. 6 and 7. We can see that for all times the single pulses produce much less radiation than the two lasers together. The effect is more than just additive. There seems to be a great synergism in intensity. This is consistent with production of carbon SWNTs, where the two-laser-pulse production rate is much greater sum of the single-pulse production rates. Apparently, the greater intensity of C_2 in the plume can be correlated with the production rate of SWNTs. We can see in Fig. 7 that as time progresses, the intensity of all plumes decreases. More will be discussed about the time evolution of the plumes in the following sections.

In Figs. 4-7 we see an underlying continuum that has a maximum at about 400 nm that is not completely understood. The underlying continuum may be due to radiation from C_3 and to particulate continua. At short wavelengths it is most likely due to C_3 . However, in other low pressure carbon laser ablation experiments Rohlfsing¹³ attributes a similar looking spectrum to Rayleigh particles and C_2 ($C^1\Pi_g - A^1\Pi_u$). [In some of our spectra we do see some weak features that could be peaks from C_2 ($C^1\Pi_g - A^1\Pi_u$) transitions.] At very low pressures, Monchicourt¹⁴ attributes spectra in this region to C_3 ($\Sigma_g^+ - \Pi_u$). Since we have not calculated the C_3 spectrum for our conditions we have not been able to confirm that what we observe in the vicinity of 400 nm is C_3 . However, the measured absorption cross section profiles of C_3 ($X^1\Sigma_g^+ - A^1\Pi_u$) by Cooper and Jones,¹⁵ in the temperature range determined here, are consistent with our measurements. Likewise, Mann¹⁶ attributed the spectra seen in a carbon/argon furnace in the neighborhood of 400 nm to the C_3 comet bands.

The significant continuum underlying the C_2 Swan bands is not well understood. It may be due to particles of carbon and/or catalyst smaller than the wavelength of light. However, the spectral distribution is not understood. We have calculated black body and Rayleigh particle emission¹⁷ curves, but there does not seem to be a temperature that would yield good agreement over the entire spectral range. As the laser ablates the target and forms a plasma plume, it is possible that electrons may be created that recombine to radiate free-bound continua. Calculations were made of $C^+ - e^-$ continua for a range of temperatures. These calculations do not seem to support this hypothesis because the spectral distribution is not consistent at low wavelengths. The measured spectra indicate a significant falloff at low wavelengths, with the intensity going to almost zero at about 310 nm. This falloff is not seen in the calculated spectra at any temperature.

Transient Emission Measurements

Transient measurements of emission at various wavelengths associated with peaks in the spectra were made to enable an assessment of the kinetics of plume development

and to help understand the buildup and decay of species. These time dependent intensities were obtained at various wavelengths with a spectral bandwidth of 6.25 nm. A summary of the intensity history measurements taken at various wavelengths is given in Fig. 8. For each wavelength the intensities are normalized by the maximum value that occurs between 100 and 1200 ns. The duration of these measurements is about 80 μ s. All wavelengths except those at 350 nm and 400 nm correspond to peaks in the Swan band spectrum. The peak at 400 nm, as well as the radiation at 350 nm may correspond to C_3 , in which case we see a different rate of production and decay of C_3 as compared with C_2 . All of the traces contain some background from other species or particles. Unfortunately, for the time being, we can only make some suggestions as to their identity.

In Fig. 8 we see that after the initial transient there are three distinct regions of decay of the intensity for most wavelengths. One region occurs from about 1.6 to 6.0 μ s, another from about 12 to 20 μ s, and the last appears to be from about 30 to at least 80 μ s. Characteristic decay times were determined from curve fits of the transient data over these times and are given in Table 1. The first time period may correspond to chemical reactions and to cooling of the plume. The second probably corresponds to reactions that consume C_2 and C_3 . The last period probably is a combination of loss of C_2 and C_3 and a

Table 1 Characteristic decay times in microseconds for three regions and eight wavelengths

<i>Wavelength, nm</i>	<i>1.6 to 6.0 μs</i>	<i>12 to 20 μs</i>	<i>30 to 80 μs</i>
	<i>Early</i>	<i>Late</i>	<i>Particle</i>
	<i>Reaction</i>	<i>Reaction and</i>	<i>Cooling</i>
	<i>Zone</i>	<i>Cooling Zone</i>	<i>Zone</i>
350	8.41	30.6	27.6
400	13.2	29.1	17
435	9.31	23.3	16.7
468	12.5	26.3	11.3
510	13.4	27.3	12.3
556	9.29	22.1	12.2
600	6.68	22.1	15.2
611	7.11	20.0	16.0

drop in temperature of particles. These decay times are much longer than the radiative lifetime of the Swan bands of 120 ns. Therefore we are seeing a change in the number and/or temperature of the radiating species.

The first 2.5 μ s of the history is seen in Fig. 9, where the 350 nm measurement shows high relative intensity spike very soon after the laser pulse. It is followed by a rise to a peak at 400 ns and then drops quickly to 20% of the peak by 1700 ns. This suggests that the radiation at 350 nm may be due to continuum from free-bound transitions early on, then C_3 or other species later.

In Fig. 10 we see time dependent ratios of intensities taken at various wavelengths for the span of time up to 80 μ s. Variations in decay rate (humps) of the intensities at various wavelengths (Fig. 8) do not appear in the ratios (or are rather subdued). This implies that we are looking at only one species and that we do not have an increase then a

decrease of, say, C_2 . If the radiation were from different species this behavior would imply that they vary together in the same way; thus one depends on or is associated with the other. Also, since we see there are no humps in the ratio associated with various Δv bands of C_2 it is very likely that the temperature does not vary much. The ratio of 468 nm to 510 nm is almost constant from 4 μs until about 20 μs . This implies that the vibrational temperature is relatively constant during that interval. In the temperature history determined from intensity integral ratios we saw that there was not much variation in temperature during this time period. After that the ratio decreases until about 55 μs .

The fact that the ratio of intensities of 350 to 510 nm increases from 7 μs onward is not understood, especially after about 50 μs . It may be associated with a disappearance of C_2 relative to particulates. This same behavior is seen in the ratio of 610 to 510 nm.

In Fig. 10 we see the initial transient of the intensities. We see that there is a very fast rise of the shortest wavelength measured (350 nm) which falls very rapidly compared with the reference wavelength (510 nm). The time that the intensities reach a maximum varies as a function of wavelength. See Fig. 11. Wavelengths associated with the C_2 Swan bands tend to peak around 800 to 1100 ns. At an estimated speed of sound of about 1500 m/s (based on a temperature of 5000 K) the distance the plume could travel would be about 1.5 mm. This is consistent with the location of the observation point from the target surface. The earlier time for the short wavelength (350 nm) may be due to a continuum excited by precursor (fast) electrons. Since we have not identified the source of the continuum in this range we can only speculate about why the shorter wavelengths tend to peak earlier than the longer wavelengths.

Estimates of vibrational temperatures are possible that show the relaxation of temperature with time. The ratio of vibrational peaks in the spectrum depends on the vibrational temperature. Using a technique described in Ref. 18, theoretical spectra were calculated at various temperatures; and ratios of integrals over short intensity ranges were found as a function of temperature. In particular we chose to use the ratio of intensity integrals in the vicinity of the vibrational peaks (1,0) and (0,0) of the C_2 Swan band ($d^3\Pi_g - a^3\Pi_u$). Integrated intensities over the wavelength ranges 465.04-475.87 nm and 509.87-519.07 nm, were determined, with an estimated underlying continuum subtracted. The ratios of measured intensities were then compared with integral ratios calculated as a function of temperature; and from that the temperatures were estimated. The first point covers a time interval from 0.4 μs to 10.4 μs . During that time there is a significant variation in the intensities. Therefore, the inferred temperature during that interval is an approximate average. The temperature histories are shown in Fig. 12. Note that the temperatures decrease slowly with time over the range covered, and that the temperature is highest with both laser pulses together. The temperatures for the green single pulse is higher than for the IR single pulse.

The surface temperature of the target may be greater with two close pulses leading to additional ablation. Yudasaka, et al.¹⁹ made measurements of nanotube production in a similar laser ablation facility at various pressures from about 0.5 kPa to about 67 kPa. They found that higher pressures resulted in increased production of carbon single wall nanotubes. They proposed that this was due to greater evaporation of catalysts due to higher temperature surfaces at higher pressure. In the present experiments the two-laser pulse operation produces more SWNT; and we speculate that the surface temperature is

higher. We also see that the C₂ Swan bands are much more intense; and therefore, we attribute the increased production to a greater amount of ablation of carbon. This does not necessarily contradict the conclusion of Yuasaka, et al. that evaporation of catalysts may be a factor in their experiments, since at our higher pressure, we were already in a regime in which nanotubes were produced for all laser combinations.

We have attempted to subtract the continuum in the measurements for a better comparison with the calculated spectra. Fig. 13 is a comparison of calculated spectra with measured spectra from which the strong continuum background was subtracted. We see differences in the measured and calculated spectra at high vibrational/rotational energy levels toward the violet side of the band heads. The continuum was estimated by choosing the points at the minima between peaks in the Swan bands. These points were then curve fit and interpolated values were subtracted from the measured spectra. It can be seen that the resultant spectrum measured at 400 ns after the laser pulses does not match calculated spectra over the entire range for any temperature. (The same disagreement was seen in the spectra for other delay times.) This indicates a significant amount of nonequilibrium in the vibrational states. This may be due to high level states being populated by recombination of carbon atoms (chemiluminescence) rather than by thermal excitation. We do see fair agreement at a temperature between 4000 K and 5000 K in the wavelength range from about 450 nm to 520 nm. This is at variance with the intensity ratio technique which showed that the temperature is closer to 3500 K. It is quite likely that the difference is due to dominance of the upper vibrational states by recombination that leads to a nonequilibrium vibrational population. This hypothesis is also supported by the nature of the distribution of intensities in the $\Delta v = -1$ system in the wavelength range 530 to 565 nm and in the $\Delta v = -2$ system in the wavelength range 580 to 620 nm. Further investigation is warranted.

Conclusions

We have presented the first known optical diagnostics measurements taken in a laser ablation plume for the production of single wall carbon nanotubes. Photographs indicate that the luminous plume is only a few millimeters in diameter and extends a few millimeters from the surface of the target. A glow is seen where the laser illuminates the upstream particles in the flow tube. This is attributed to luminous particles heated by the laser beams.

Spectral measurements of the plume emission indicate that the primary emission is from the C₂ Swan band system. There is also a significant continuum underlying these bands that is probably from particulate radiation. However, the intensity distribution does not clearly indicate that this is gray body radiation. It also deviates from Rayleigh particle emission. We also see a feature in the spectrum and covering a range of 310 nm to at least 430 nm, peaking at about 400 nm that appears to be C₃. No atomic lines were seen in the wavelength range measured. Temperatures at several time points were inferred from measured intensity ratios of integrals of Swan band features. The temperatures showed a dependence on the combination of laser pulses, with both laser pulses resulting in higher temperatures and the 532 nm laser producing higher temperatures than the 1064 nm laser, even though the pulse energies were the same. The range of temperatures during the first 30 microseconds was estimated to be from 2500 K to 3800 K. However, estimates of

temperatures from the shape of the $\Delta v=-1$ and $\Delta v=-2$ bands were higher. The difference between the two techniques may be due to nonequilibrium associated with high vibrational states being produced by recombination rather than thermal excitation.

Higher intensities were seen with both laser pulses as compared with only single pulses. This correlated with the amount of single wall carbon nanotubes produced. There seems to be a synergistic behavior with two laser pulses separated in time by 50 ns.

Transient measurements were made at several wavelengths which showed that peak intensities occur at about 800-1100 ns for the C_2 band heads, whereas, radiation at 350 nm peaks much earlier, suggesting a quite different phenomenon is causing radiation at this wavelength. The overall shape of the transient curves is similar for the C_2 band heads; and the curves for 350 nm and 400 nm appear quite different from the others. In fact the normalized 350 nm curve becomes greater than the others after about 60 μs , implying that the C_2 radiation is disappearing, whereas, other radiation, e. g., continuum from particles or other species remains.

In the future, additional information may be obtained from spectral analyses in regions of the spectrum not included in this study. Also, more detailed higher resolution investigation of some of the molecular bands may enable us to obtain a better picture of vibrational populations, and hence, the existence of a temperature or nonequilibrium. Also, spectral data collected as a part of a parametric study to optimize SWNT production is being analyzed and will be presented at a later date.

Acknowledgments

The authors gratefully acknowledge Professor Richard Smalley of Rice University in his encouragement of our project, Dr. Lubert Léger in his leadership in establishing the nanotube project at the Johnson Space Center and Mr. William Holmes for his invaluable help in data collection. Thanks are also due to Dr. Charles Hakes, Mr. Jeremy Jacobs, and Mr. Joe Victor in setting up the experimental apparatus, to Dr. Larry Lewis for initial parametric study of the optical diagnostics, and to Dr. Bradley Files for his continued encouragement.

References

-
- ¹ Ajayan, P. M., Stephan, O., Redlich, Ph., and Coltrex, C., "Carbon Nanotubes as Removable Templates for Metal Oxide Nanocomposites and Nanostructures," *Nature*, Vol. 375, 1995, pp. 564-567.
 - ² Yakobson, B. I., and Smalley, R. E., "Fullerene Nanotubes: $C_{1,000,000}$ and Beyond," *American Scientist*, Vol. 85, 1997, pp. 324-337.
 - ³ Frank, S., Poncharal, P., Wang, Z. L., and de Heer, W. A., "Carbon Nanotube Quantum Resistors," *Science*, Vol. 280, June 12, 1998, pp. 1744-1746.
 - ⁴ Dillon, A. C., Jones, K. M., Bekkendahl, T. A., Kiang, C. H., Bethune, D. S., and Heben, M. J., "Storage of Hydrogen in Single-Walled Carbon Nanotubes," *Nature*, Vol. 386, 1997, pp. 377-379.
 - ⁵ Journet, C., Maser, W. K., Bernier, P., Loiseau, A., Lamy de la Chapelle, M., Lefrant, S., Deniard, P., Lee, R., and Fischer, J. E., "Large Scale Production of Single Wall Carbon Nanotubes by the Electric Arc Technique," *Nature*, Vol. 388, 21 August 1998, pp. 756-758.
 - ⁶ Iijima, S. and Ichihashi, T., "Single-shell Carbon Nanotubes of 1-nm Diameter," *Nature*, Vol. 363, 1993, pp. 603-605.
 - ⁷ Guo, T., Nikolaev, P., Thess, A., Colbert, D. T., Smalley, R. E., "Catalytic growth of single-walled nanotubes by laser vaporization," *Chemical Physics Letters*, Vol. 243, 1995, pp. 49-54.

-
- ⁸ Thess, A., Lee, R., Nikolaev, P., Dai, H.; Petit, P., Robert, J., Xu, C., Lee, Y. H., Kim, S. G., Rinzler, A. G., Tomanek, D., Fisher, I. E., and Smalley, R. E., "Crystalline Ropes of Metallic Carbon Nanotubes" *Science*, Vol. 273, 1996, pp. 483-487.
- ⁹ Terrones, M., Grobert, N., Zhang, J. P., Terrones, H., Olivares, J., Hsu, W. K., Hare, J. P., Cheetham, A. K., Kroto, H. W., and Walton, D. R. M., "Preparation of Aligned Carbon Nanotubes Catalysed by Laser-etched Cobalt Thin Films," *Chemical Physics Letters*, Vol. 285, 1998, pp. 299-305.
- ¹⁰ Cheng, H. M., Li, F., Su, G., Pan, H. Y., He, L. L., Sun, X., and Dresselhaus, M. S., "Large-scale and Low-cost Synthesis of Single-walled Carbon Nanotubes by the Catalysis Pyrolysis of Hydrocarbons," *Applied Physics Letters*, Vol. 72, 1998, pp. 3282-3284.
- ¹¹ Files, B. S., "Applications of Carbon Nanotubes for Human Space Exploration," Proceedings of the International Conference on Integrated Nano/Microtechnology for Space Applications, November 1-6, 1998.
- ¹² Danylewych, L. L. and Nicholls, R. W., "Intensity Measurements on the C_2 ($d^3\Pi_g-a^3\Pi_u$) Swan Band System," *Proceedings of the Royal Society of London A*, Vol. 339, 1974, pp. 197-212.
- ¹³ Rohlfing, E. A., "Optical Emission Studies of Atomic, Molecular, and Particulate Carbon Produced from a Laser Vaporization Cluster Source," *J. of Chemical Physics*, Vol. 89, No. 10, 15 Nov. 1988, pp. 6103-6112.
- ¹⁴ Monchicourt, P., "Onset of Carbon Cluster Formation Inferred from Light Emission in a Laser-Induced Expansion," *Physical Review Letters*, Vol. 66, No. 11, 18 March 1991, pp. 1430-1433.
- ¹⁵ Cooper, D. M. and Jones, J. J., *J. Quantitative Spectroscopy and Radiative Transfer*, Vol. 22, 1979, pp. 201-208.
- ¹⁶ Mann, D. M., "A Possible First Step in Carbon Particle Formation: $C_2 + C_3$," *J. Applied Physics*, Vol. 49, No. 6, June 1978, pp. 3485-3489.
- ¹⁷ Bohren, C. F. and Huffman, D. R., *Absorption and Scattering of Light by Small Particles*, John Wiley & Sons, New York, 1993.
- ¹⁸ Scott, C. D., Blackwell, H. E., Arepalli, S., and Akundi, M. A., "Techniques for Estimating Rotational and Vibrational Temperature in Nitrogen Arcjet Flow," *Journal of Thermophysics and Heat Transfer*, Vol. 12, No. 4, October-December, 1998, pp. 457-464.
- ¹⁹ Yudasaka, M., Komatsu, T., Ichihashi, T., Achiba, Y., and Iijima, S., "Pressure Dependence of the Structures of Carbonaceous Deposits Formed by Laser Ablation on Targets Composed of Carbon, Nickel, and Cobalt," *J. Physical Chemistry B*, Vol. 102, 1998, pp. 4892-4896.

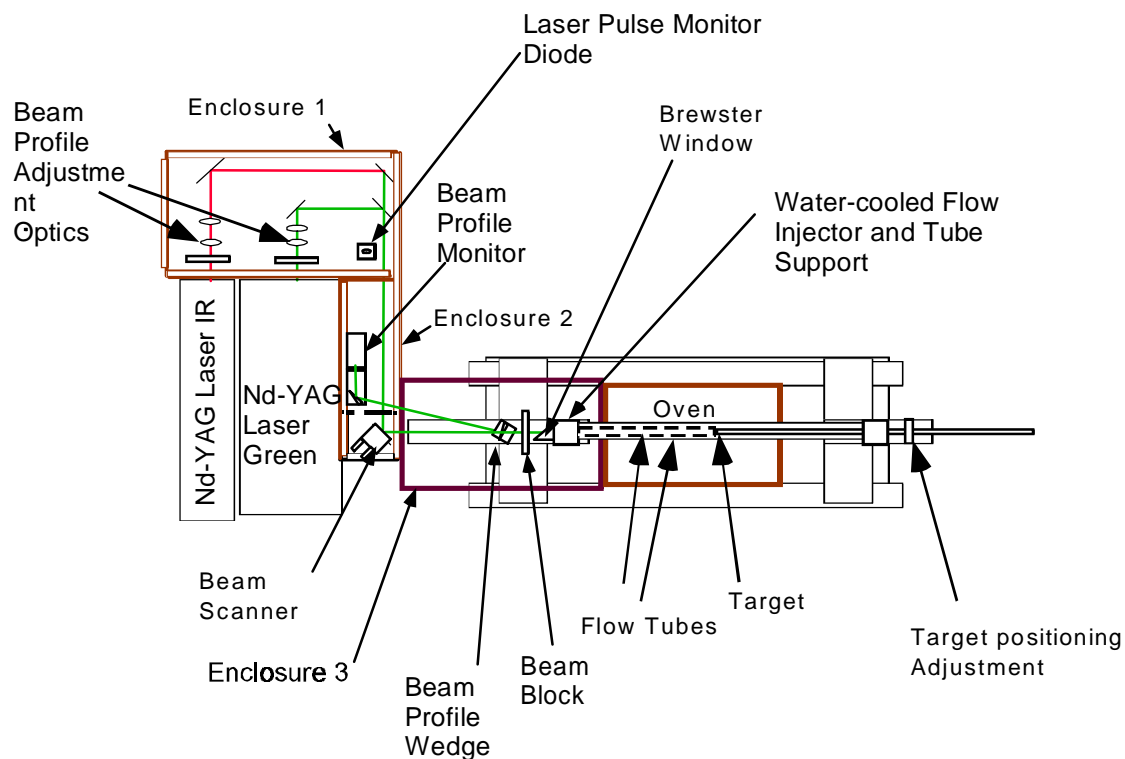


Fig. 1 Layout of laser ablation process for carbon single wall nanotube production.

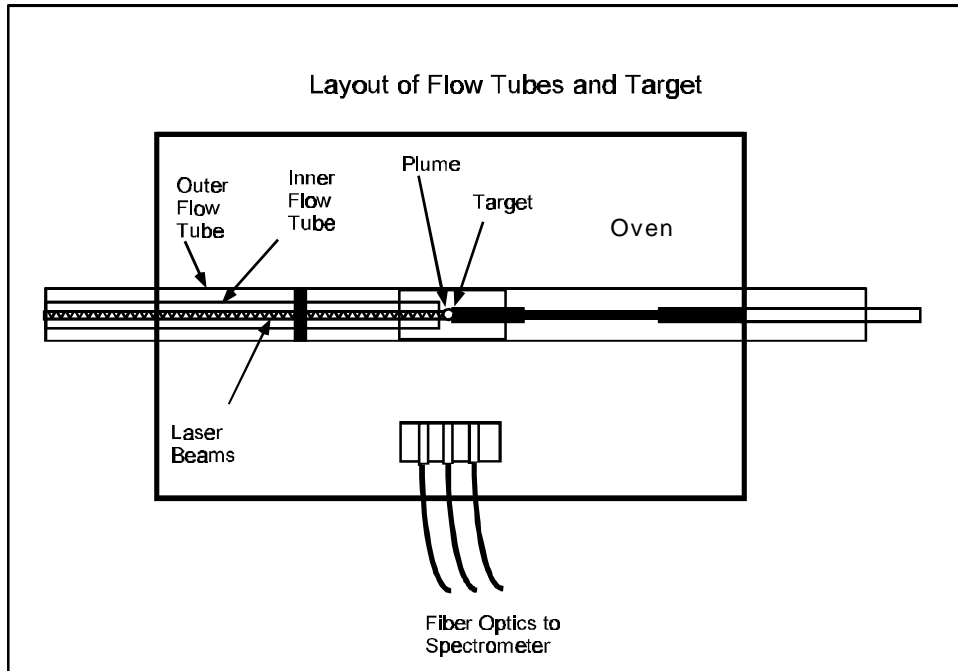


Fig. 2 Configuration of flow tubes and target showing laser beams, plume and fiber optic light collectors

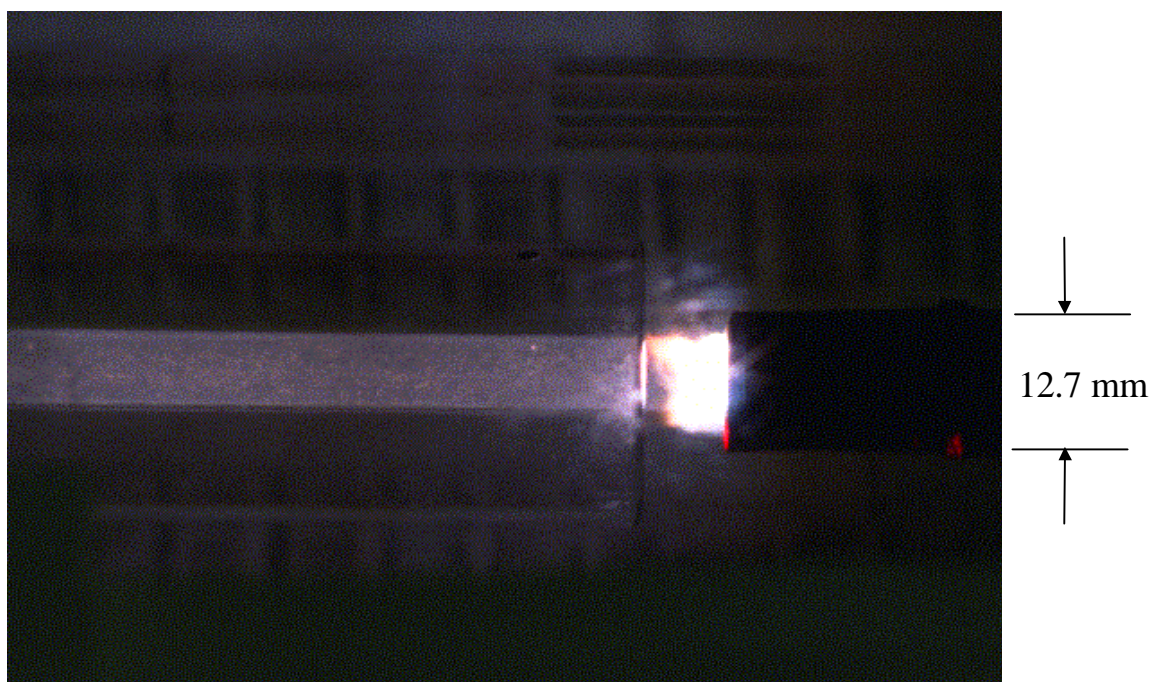


Fig. 3 Photograph of reaction zone inside 1-inch tube showing laser induced radiation. Photograph taken using notch filter to eliminate scattered laser light.

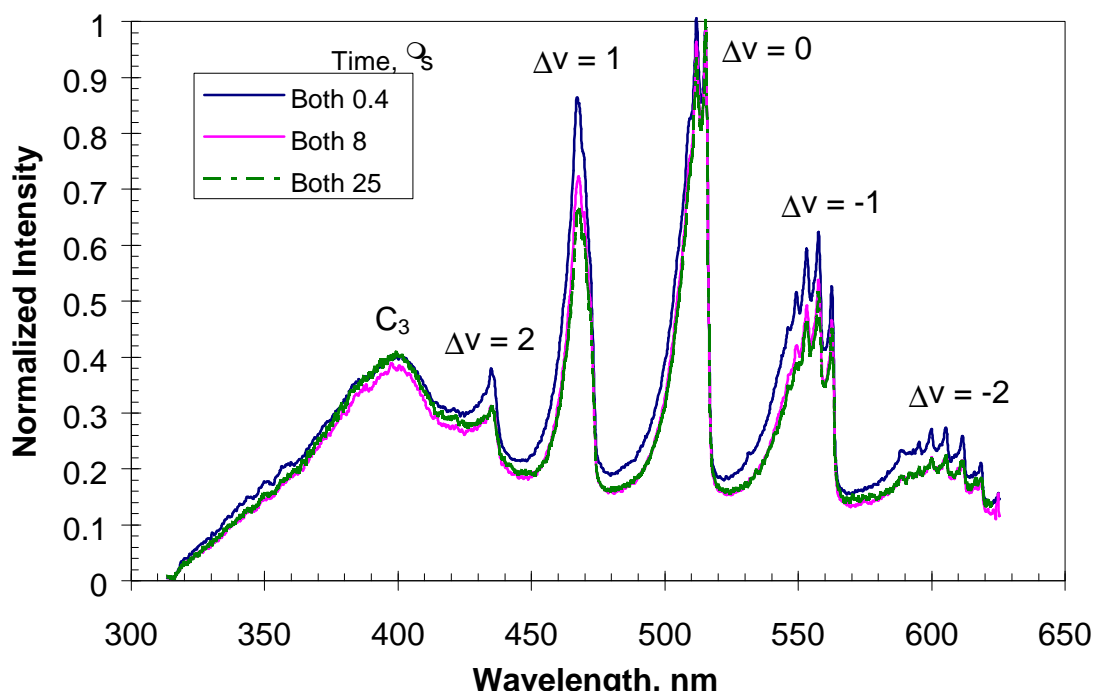


Fig. 4 Normalized spectral distributions obtained in laser ablation plume at various times after laser pulses with identification of peaks associated with C_2 Swan bands and C_3 . Both lasers are fired.

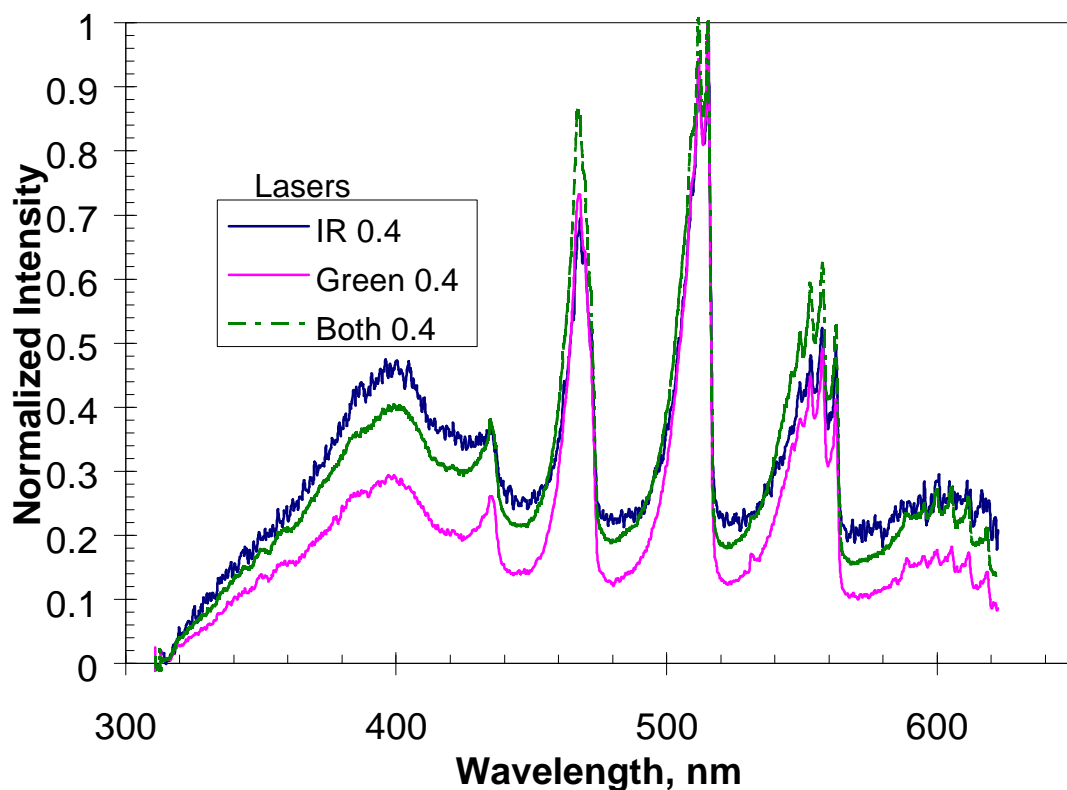


Fig. 5 Normalized spectra taken 0.4 ms after laser pulses, with duration of 10 ms, showing C_2 Swan bands and underlying continua. Comparison is made for various laser pulses.

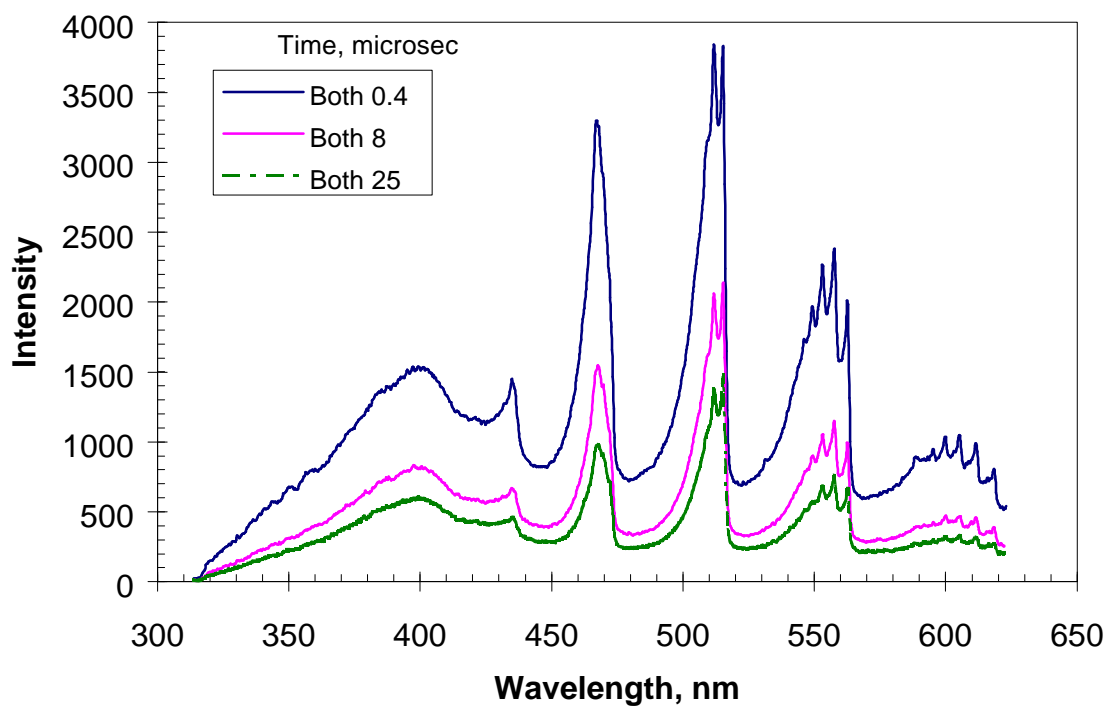


Fig. 6 Spectrum taken with 10 μ s gate at three times following the laser pulses. Both lasers are fired 50 ns apart.

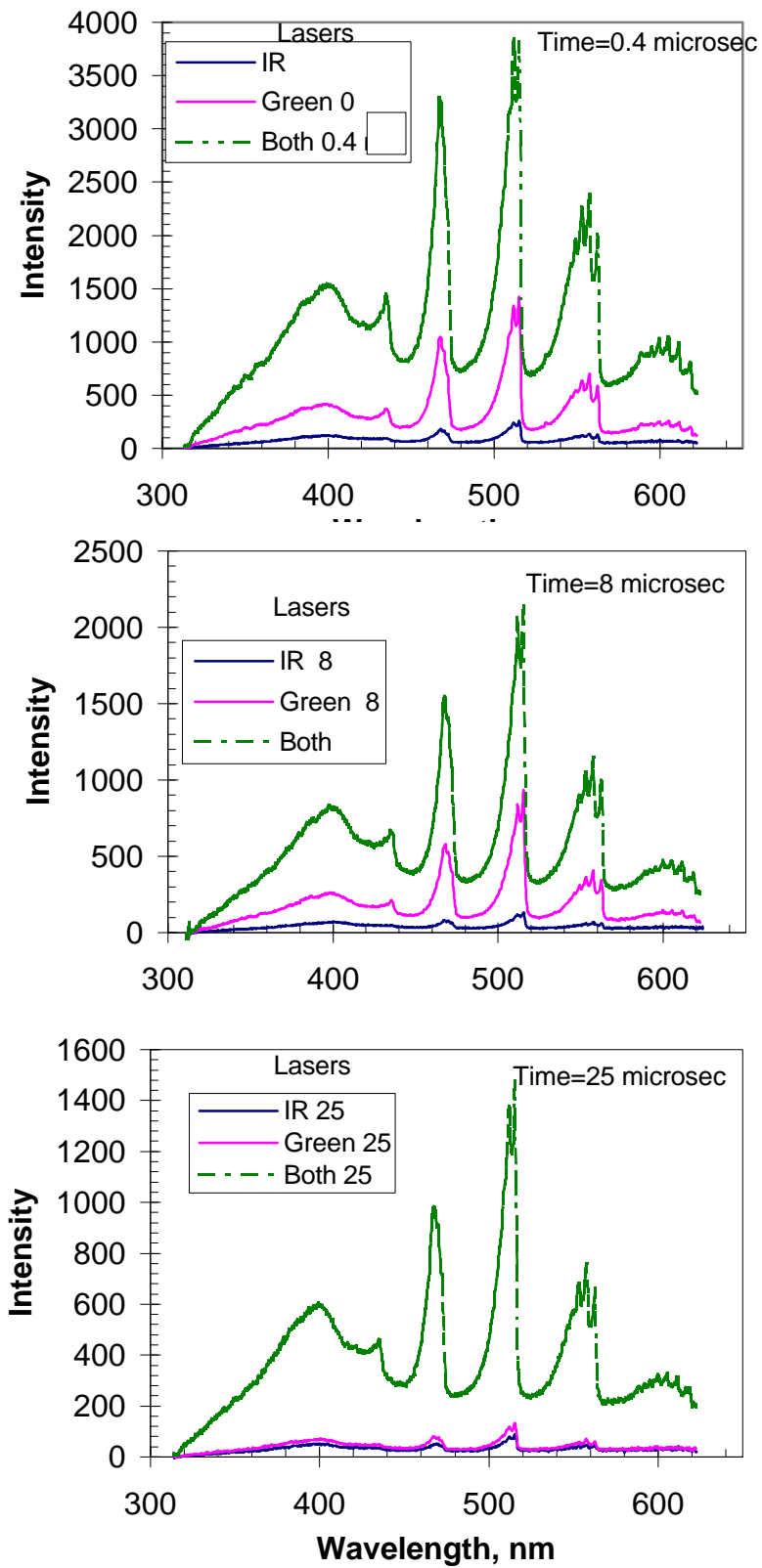


Fig. 7 Un-normalized spectra taken 0.4, 8, and 25 μ s after laser pulses for all laser pulses.

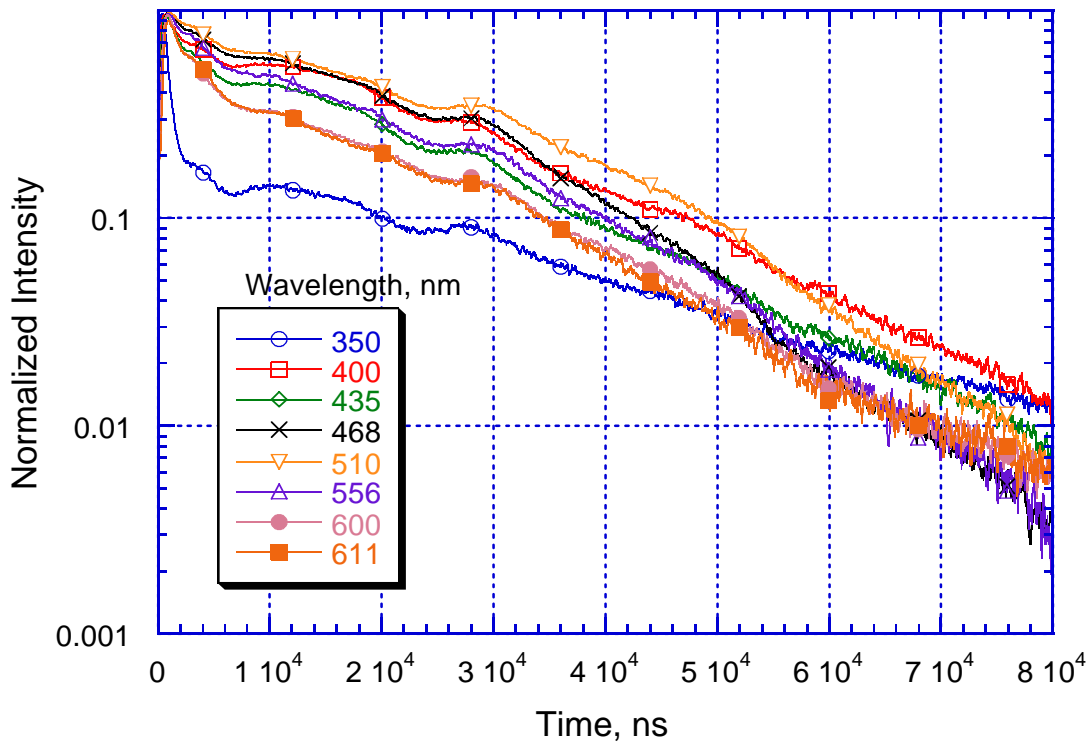


Fig. 8 Normalized and then smoothed transient intensities at various wavelengths from 0 to 80 μ s.

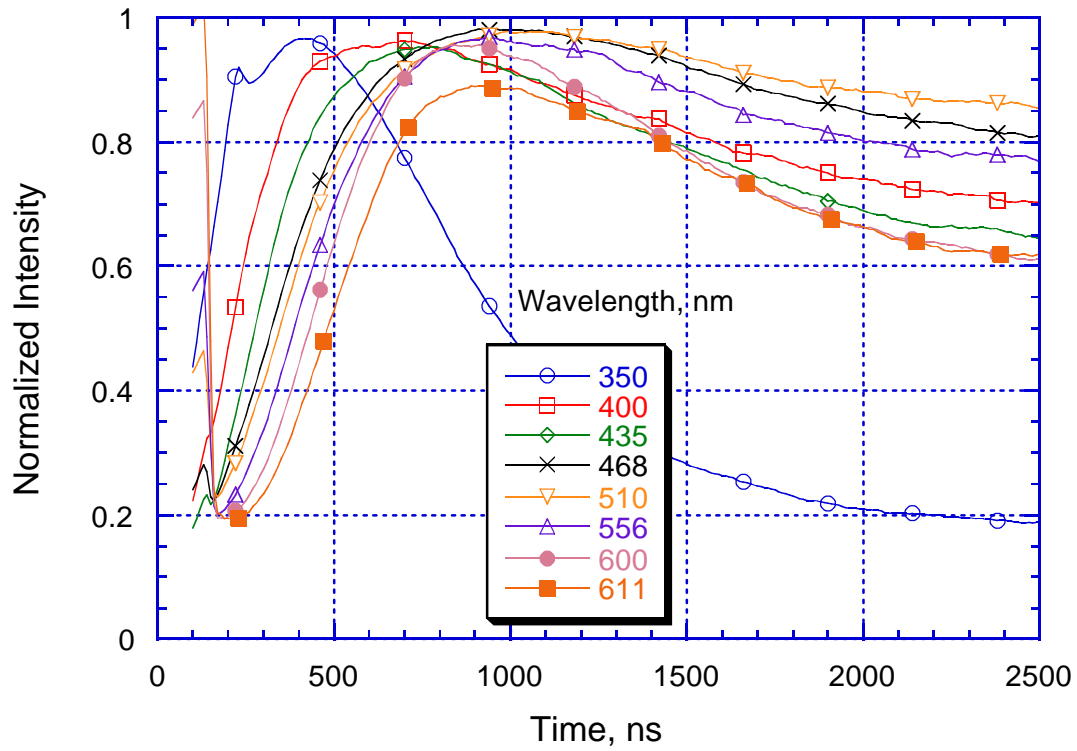


Fig. 9 Normalized and then smoothed transient intensities at various wavelengths from 0.1 to 2.5 μ s.

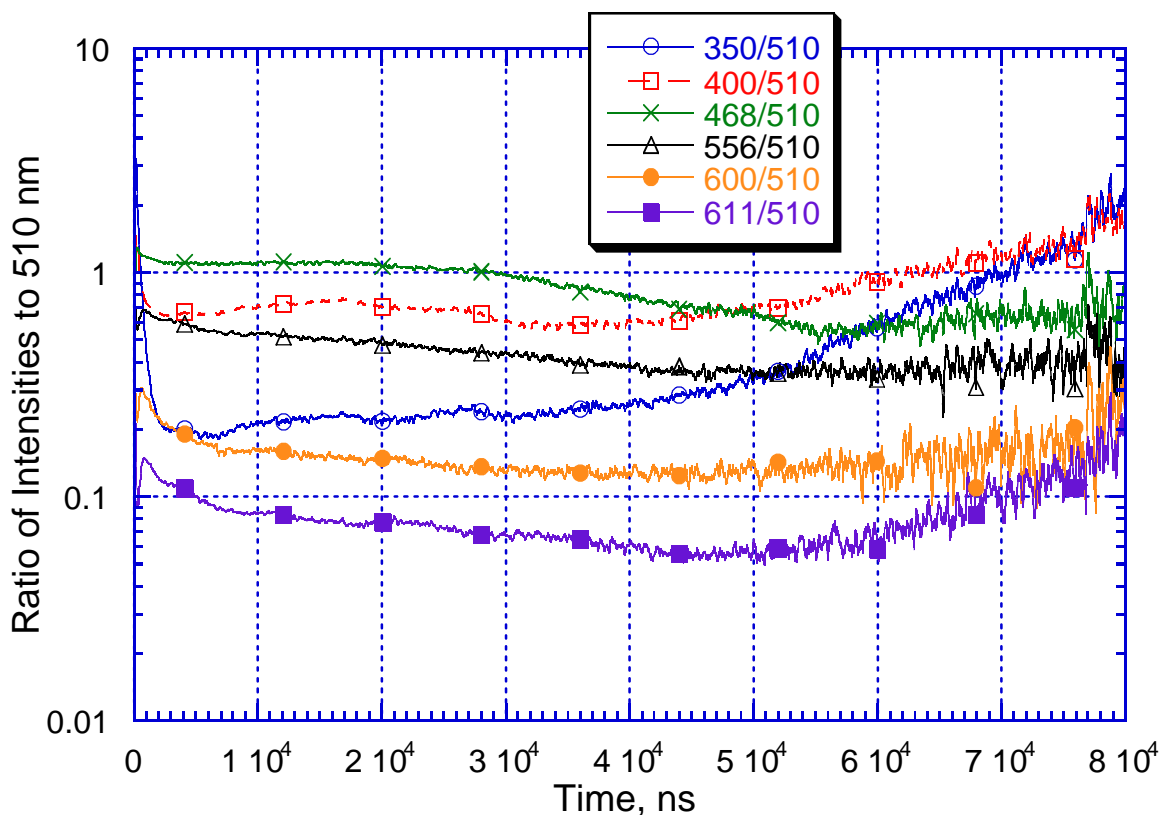


Fig. 10 Normalized and smoothed ratios of transient intensities covering 80 μ s. The reference wavelength is 510 nm, which is the band peak associated with the $\Delta v=0$ transitions of the C_2 Swan band.

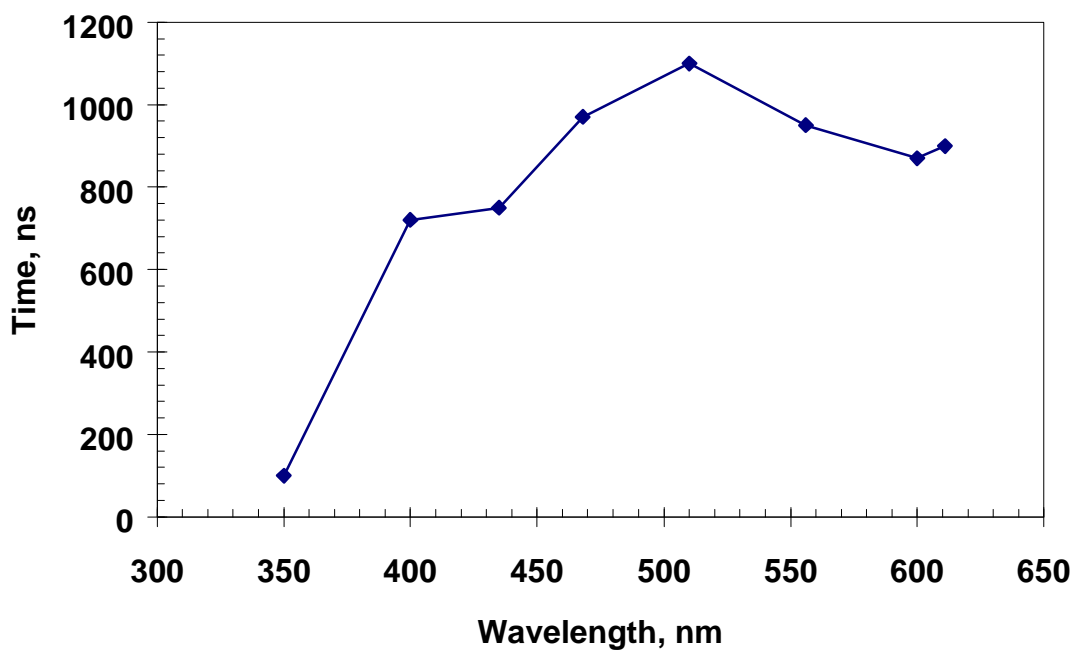


Fig. 11 Time to peak intensity in the transient spectra of selected wavelengths.

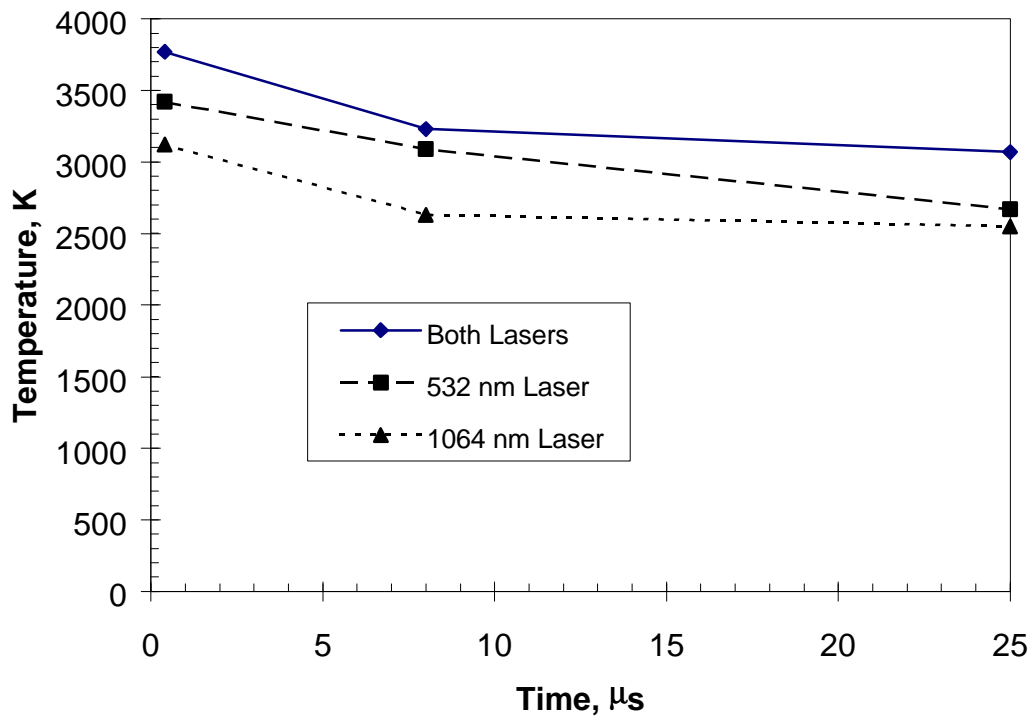


Fig. 12 Temperatures in plume determined from C_2 Swan band intensity ratios of (1,0)/(0,0) bands.

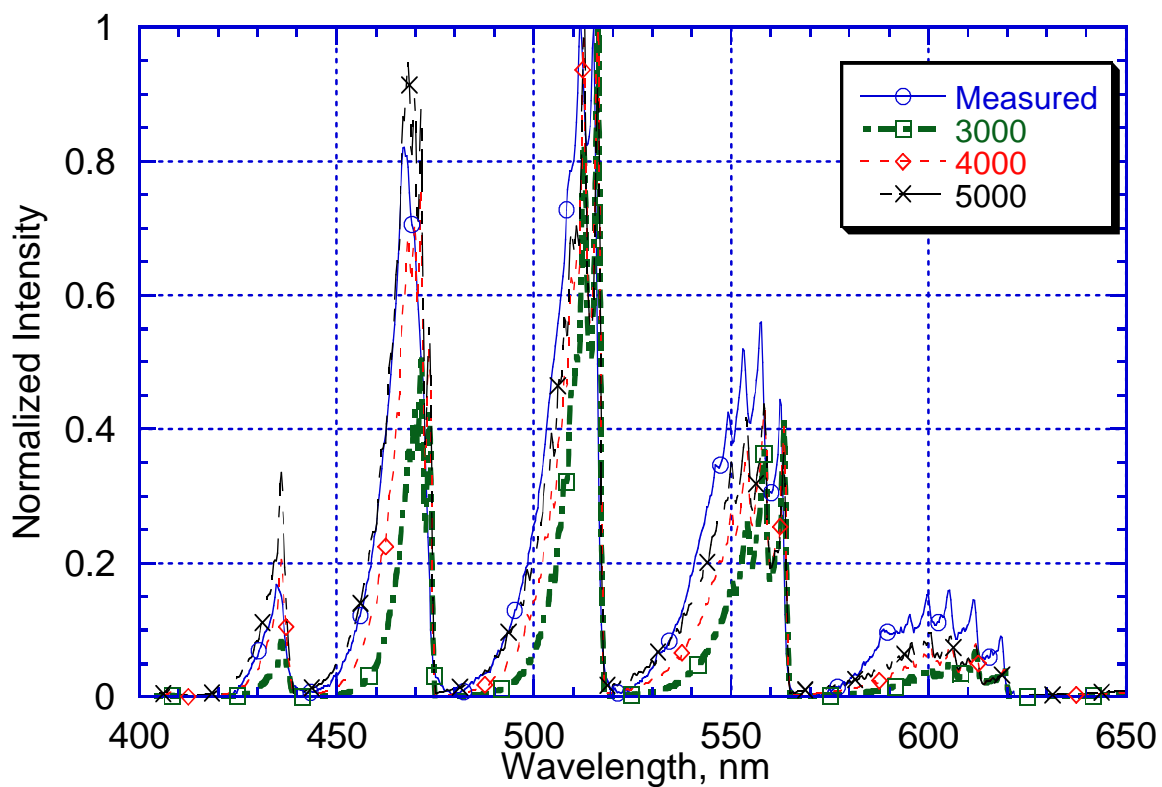


Fig. 13 Measured spectrum with estimated continuum subtracted compared with calculated C_2 Swan bands at three temperatures. Measurement at 400 ns with duration of 10 μ s with both laser pulses.